Int.J.HIT.TRANSC:ECCN.Vol.7: Issue 2A (2021) Page 35-60 ISSN: 0973-6875

Available Online at www.hithaldia.in/locate/ECCN
All Rights Reserved

ORIGINAL CONTRIBUTION

Static Deflections, Forces and Moments Of Stiffened Conoidal Roof Shells Under Point Load – A Finite Element Approach

[1]Sasank sekhar Hota and [2]Dipankar Chakravorty

[1]Research scholar, Department of Civil Engineering, Jadavpur University, Kolkata- 700 032, India

[2] Reader, Department of Civil Engineering, Jadavpur University, Kolkata- 700 032, India

ABSTRACT

A review of literature reveals that information regarding static deflections; forces and moments of stiffened conoidal shells are missing although these shell forms are very important industrially. Here the present investigation aims to fulfill the gap using a stiffened shell element combining an eight noded doubly curved shell element and a three noded curved beam element. Benchmark problems are solved to check the validity of the approach and different problems of simply supported and clamped conoids with various stiffener arrangements are solved to obtain the different static shell actions under central concentrated load. Typical results of different shell actions are also furnished by varying the stiffener depth and eccentricity with respect to the shell midsurface. The results will be of great help to practicing engineers. Relative efficiencies of two different shell options with different boundary conditions and number of stiffeners are compared through a proposed performance matrix. The paper ends with a number of conclusions drawn from the present study.

KEYWORDS: stiffened conoidal shell, finite element analysis, shell actions, concentrated load, simply supported, clamped.

.

1. INTRODUCTION

Doubly curved anticlastic conoidal shells are ruled surfaces and hence are easy to cast and fabricate. They are aesthetically appealing, can permit entry of north light and are preferred as roofing units in many practical situations particularly in food processing and medicine industries where large column-free lighted spaces are needed. Like any other general shell form these conoidal shell surfaces need to be stiffened particularly when point loads are imposed and in cases where cutouts are introduced on these surfaces.

Research about conoidal shells dates back to the seventh decade of the last century when Hadid (1964) used a combined variational method for static analysis of clamped elastic unstiffened conoidal shells. He also applied the integral equation technique to investigate the bending of simply supported and clamped conoidal shells. A rectangular curved finite element was employed by Brebbia and Hadid (1971) to explore the static behaviour of clamped conoidal shells. The finite element method was also employed by Choi (1984) and later by Ghosh and Bandyopadhyay (1989) and Das and Bandyopadhyay (1993) to investigate the bending characteristics of conoids. Later Chakravorty et al. (1995) and (1996) employed the finite element approach for free vibration study of composite unstiffened conoidal shells for different boundary conditions.

The volume of literature that accumulated upto 1995 about stiffened shells was reviewed by Sinha and Mukhopadhyay (1995) where they clearly concluded that stiffened shell panels in general and doubly curved panels in particular were not figuring in literature in large numbers. Recently Nayak and Bandyopadhyay (2002a)

*Corresponding Address: dchakravorty@vsnl.net

and (2002b) reported the natural frequencies of stiffened shallow shells including the conoids in two different papers with the second paper dealing with stiffened conoidal shells only. In another recent paper Prusty and Satsangi (2001) solved the bending problems of stiffened spherical shell panels but reported the deflections only.

It is evident from the study of the literature that unstiffened conoids received some attention no doubt, but the few reports which deal with stiffened conoidal shells are about free vibration only. To utilize these stiffened conoidal shell forms (Fig.1) confidently as civil engineering roofing units, static analysis apart from vibration studies is to be carried out. Feeling this necessity the present work endeavours to study comprehensively the deflections, force and moment resultants of stiffened conoidal shells under central concentrated load considering both simply supported and clamped boundary conditions employing a cubic triangular shell element as the master element and a 3-noded stiffener as the slave element. The method of analysing this stiffened structure by an orthotropic model (Timoshenko& Kriger) is not appropriate as stiffeners are disposed on the shell surface not at close intervals. As several triangular stiffened models exist previously it is pertinent here to establish the advantage possessed by this model over them.

2. MATHEMATICAL FORMULATION BY FINITE ELEMENT

Shell element

An eight noded curved quadratic isoparametric element (Fig2.a) is used to model the shallow, thin shell surface having five degrees of freedom per node (Fig 3) including two inplane displacements (u, v), one transverse displacement (w) and two rotations (α, β).

The shape functions which are used to interpolate both the displacement field and the element geometry are as below:

[1] $N_i = (1+\xi\xi_i)(1+\eta\eta_i)(\xi\xi_i+\eta\eta_i-1)/4$ for i = 1, 2, 3, 4

$N_i = (1+\xi\xi_i)(1+\eta^2)/2$ for i = 5, 7

$N_i = (1+\eta\eta_i)(1-\xi^2)/2$ for i = 6, 8

where i denotes the node number.

The generalized displacement vector of an element is expressed in terms of the shape functions and nodal degrees of freedom as:

[2] $$\{u\} = [N]\{d_n\} = \sum_{i=1}^{8} N_i [I]_{5\times5} \{u_i, v_i, w_i, \alpha_i, \beta_i\}^T$$

For an isotropic, homogeneous, linearly elastic, thin, shallow shell the constitutive relation is given below (vide list of notations in appendix and Fig. 4).

[3] $$\{F\} = [D]\{\varepsilon\}$$

where $\{F\} = \{N_x, \quad N_y, \quad N_{xy}, \quad M_x, \quad M_y, \quad M_{xy}, \quad Q_x, \quad Q_y\}^T$

$$= \int_{-h/2}^{+h/2} \left\{ \sigma_x, \quad \sigma_y, \quad \tau_{xy}, \quad \sigma_x.z, \quad \sigma_y.z, \quad \tau_{xy}.z, \quad \tau_{xz}, \quad \tau_{yz} \right\}^T dz$$

The elasticity matrix [D] has the following form.

$$[D] = \frac{Eh}{1-\upsilon^2} \begin{bmatrix} 1 & & & & & & & \\ \upsilon & 1 & & & & & & \\ 0 & 0 & \frac{1-\upsilon}{2} & & \textit{symmetric} & & & \\ 0 & 0 & 0 & \frac{h^2}{12} & & & & \\ 0 & 0 & 0 & \frac{\upsilon h^2}{12} & \frac{h^2}{12} & & & \\ 0 & 0 & 0 & 0 & 0 & \frac{h^2(1-\upsilon)}{24} & & \\ 0 & 0 & 0 & 0 & 0 & 0 & \frac{1-\upsilon}{2.4} & \\ 0 & 0 & 0 & 0 & 0 & 0 & 0 & \frac{1-\upsilon}{2.4} \end{bmatrix}$$

Based on the modified Sander's first approximation theory for thin shells the strains are as follows:

[4] $$\left\{ \varepsilon_x, \varepsilon_y, \gamma_{xy}, \gamma_{xz}, \gamma_{yz}, k_x, k_y, k_{xy} \right\}^T = \left\{ \frac{\partial u}{\partial x}, \frac{\partial v}{\partial y} - \frac{w}{R_Y}, \frac{\partial u}{\partial y} + \frac{\partial v}{\partial x} - \frac{2w}{R_{XY}}, \alpha + \frac{\partial w}{\partial x}, \beta + \frac{\partial w}{\partial y}, 0,0,0 \right\}^T$$

$$+ z \left\{ 0,0,0,0,0, \frac{\partial \alpha}{\partial x}, \frac{\partial \beta}{\partial y}, \frac{\partial \alpha}{\partial y} + \frac{\partial \beta}{\partial x} \right\}^T$$

The radius of cross curvature (R_{xy}) and that along y-direction (R_y) may be calculated by differentiating the surface equation of the shell in the form z = f(x, y) (Fig.1). For shallow shells considered here one may use

$$\frac{1}{R_{xy}} = \frac{\partial^2 z}{\partial x \partial y} \text{ and } \frac{1}{R_y} = \frac{\partial^2 z}{\partial y^2}.$$

The strains and displacements are connected as:

[5] $$\{\varepsilon\} = [B]\{d_n\}$$

where $[B]=\sum_{i=1}^{8}\begin{bmatrix} N_{i,x} & 0 & 0 & 0 & 0 \\ 0 & N_{i,y} & \frac{-N_i}{R_Y} & 0 & 0 \\ N_{i,y} & N_{i,x} & -\frac{2N_i}{R_{xy}} & 0 & 0 \\ 0 & 0 & N_{i,x} & N_i & 0 \\ 0 & 0 & N_{i,y} & 0 & N_i \\ 0 & 0 & 0 & N_{i,x} & 0 \\ 0 & 0 & 0 & 0 & N_{i,y} \\ 0 & 0 & 0 & N_{i,y} & N_{i,x} \end{bmatrix}$

The element stiffness matrix for the shell is

[6] $$[K_{she}] = \int\int [B]^T [D][B]\, dxdy$$

The integral is converted to isoparametric coordinates using appropriate Jacobian transformation and is carried out by 2 × 2 Gauss quadrature.

Stiffener element

Three noded curved isoparametric beam elements (vide Fig.2b and 2c) are used to model the stiffeners with four degrees of freedom per node including axial and transverse displacements, flexural and torsional rotations. The stiffened shell surface is discretised in such a way so that the stiffener elements always run along boundaries of shell elements.

The shape functions for x-stiffener depend on ξ and are given below.

[7] $$N_{\xi i} = 0.5\xi\xi_i(1+\xi\xi_i) \qquad \text{for } i = 1, 3$$

$$N_{\xi i} = (1-\xi^2) \qquad \text{for } i = 2$$

The generalized displacement vector of an x-stiffener element is expressed in terms of the shape functions and nodal degrees of freedom as:

[8] $$\{u_{sx}\} = [N_{sx}]\{d_{nsx}\} = \sum_{i=1}^{3} N_{\xi i}[I]_{4\times 4}\{u_i, w_i, \alpha_i, \beta_i\}^T$$

The generalized constitutive relation for x- stiffener element can be expressed as below.

[9] $$\{F_{sx}\} = [D_{sx}]\{\varepsilon_{sx}\}$$

The force vector $\{F_{sx}\} = \{N_{sxx}, M_{sxx}, T_{sxx}, Q_{sxx}\}^T$ where $N_{sxx}, M_{sxx}, T_{sxx}, Q_{sxx}$ are the usual force, moment, torsion and shear resultants of x-stiffener element.

The elasticity matrix of x-stiffener element is given as follows:

$$[D_{sx}] = \begin{bmatrix} EA & & & \\ ES & EI & symmetric & \\ 0 & 0 & GJ & \\ 0 & 0 & 0 & \frac{GA}{1.5} \end{bmatrix}$$

where E, G, A, S, I and J are the modulus of elasticity, modulus of rigidity, cross-sectional area, first moment of area, moment of inertia and equivalent polar moment of inertia of the isotropic *x*-stiffener respectively about the reference axis which lies on the shell mid surface.

The strain vector of the *x*-stiffener is given below.

[10] $$\{\varepsilon_{sx}\} = \{\varepsilon_{sxx}, k_{sxx}, k_{sxxy}, \gamma_{sxz}\}^T = \left\{\frac{\partial u_{sx}}{\partial x}, \frac{\partial \alpha_{sx}}{\partial x}, \frac{\partial \beta_{sx}}{\partial x}, \alpha_{sx} + \frac{\partial w_{sx}}{\partial x}\right\}^T$$

The strain-displacement relationship for *x*-stiffener can be written in matrix form as:

[11] $$\{\varepsilon_{sx}\} = [B_{sx}]\{d_{nsx}\}$$

where $$[B_{sx}] = \sum_{i=1}^{3} \begin{bmatrix} N_{\xi i,x} & 0 & 0 & 0 \\ 0 & 0 & N_{\xi i,x} & 0 \\ 0 & 0 & 0 & N_{\xi i,x} \\ 0 & N_{\xi i,x} & N_{\xi i} & 0 \end{bmatrix}$$

The element stiffness matrix of *x*-stiffener is given as:

[12] $$[K_{xe}] = \int [B_{sx}]^T [D_{sx}] [B_{sx}] dx$$

The integral is transformed to isoparametric coordinate using the proper Jacobian transformation and is carried out by 2 point Gauss quadrature.

The shape functions for y-stiffener depend on η and are given below.

[13] $$N_{\eta i} = 0.5\eta\eta_i(1+\eta\eta_i) \qquad \text{for } i = 1, 3$$

$$N_{\eta i} = (1-\eta^2) \qquad \text{for } i=2$$

The generalized displacement vector of a y-stiffener element is expressed in terms of the shape functions and nodal degrees of freedom as:

[14] $$\{u_{sy}\} = [N_{sy}]\{d_{nsy}\} = \sum_{i=1}^{3} N_{\eta i}[I]_{4\times 4}\{v_i, w_i, \alpha_i, \beta_i\}^T$$

The general constitutive relation for the *y*-stiffener is given below.

[15] $$\{F_{sy}\} = [D_{sy}]\{\varepsilon_{sy}\}$$

The force vector $\{F_{sy}\} = \{N_{syy}, M_{syy}, T_{syy}, Q_{syy}\}^T$ where N_{syy}, M_{syy}, T_{syy}, Q_{syy} are usual force, moment, torsion and shear resultants of y-stiffener element.

The elasticity matrix of *y*-stiffener element is identical to that for the x-stiffener element because in the present case the sectional and material properties of the stiffeners along both the directions are taken to be identical.

The strain vector of the *y*-stiffener is given below.

[16] $$\{\varepsilon_{sy}\} = \{\varepsilon_{syy}, k_{syy}, k_{syxy}, \gamma_{syz}\}^T = \left\{\frac{\partial v_{sy}}{\partial y} - \frac{w_{sy}}{R_y}, \frac{\partial \beta_{sy}}{\partial y}, \frac{\partial \alpha_{sy}}{\partial y}, \beta_{sy} + \frac{\partial w_{sy}}{\partial y}\right\}^T$$

The strain displacement relationships for *y*-stiffener can be written in matrix form as:

[17] $$\{\varepsilon_{sy}\} = [B_{sy}]\{d_{nsy}\}$$

where $[B_{sy}] = \begin{bmatrix} N_{\eta i,y} & -N_{\eta i}/R_Y & 0 & 0 \\ 0 & 0 & 0 & N_{\eta i,y} \\ 0 & 0 & N_{\eta i,y} & 0 \\ 0 & N_{\eta i,y} & 0 & N_{\eta i} \end{bmatrix}$

Due to curvature of the *y*-stiffener the generalized displacements of the stiffener and the shell are related as follows:

[18] $\{u_{sy}\} = [T]\{u\}$

where $[T] = \begin{bmatrix} 1+\dfrac{e}{R_Y} & symmetric & & \\ 0 & 1 & & \\ 0 & 0 & 1 & \\ 0 & 0 & 0 & 1 \end{bmatrix}$

and $\{u\}$ is the appropriate portion of the displacement vector of shell excluding u.

The element stiffness matrix of the y-stiffener is given as:

[19] $[K_{ye}] = \int [T]^T [B_{sy}]^T [D_{sy}] [B_{sy}] [T]\, dy$

The integral is transformed to isoparametric coordinate using the proper Jacobian transformation and is carried out by 2 point Gauss quadrature.

Element stiffness matrix of the stiffened shell

The element stiffness matrix of the stiffened shell is obtained by appropriate matching of the nodes of the stiffener and shell elements.

[20] $[K_e] = [K_{she}] + [K_{xe}] + [K_{ye}]$

The element matrices are then assembled to obtain the global stiffness matrix $[K]$.

Element load vector

The consistent element load vector $\{P_e\}$ is given by

[21] $\{P_e\} = \int\int [N]^T \{q\} dxdy$

where, $\{q\} = \{0 \quad 0 \quad q \quad 0 \quad 0\}$ for shells under uniform transverse load. The area integral is evaluated by 2×2 Gauss quadrature after appropriate Jacobian transformation.

For point load, however, a lumped load vector is adopted.

Solution procedure

The element stiffness matrices and the element load vectors are assembled to get the global stiffness matrix and global load vector respectively on which the boundary conditions are imposed and the basic problem of static takes the form

[22] $[K]\{d\} = \{P\}$

where [K] is the global stiffness matrix, $\{d\}$ and $\{P\}$ are global generalized displacement and load vectors respectively. The above equation is solved by the Gauss elimination technique and from the global nodal displacement vector $\{d\}$ thus obtained, the element displacement vectors $\{d_n\}$ are solved. Using $\{d_n\}$, the strains and hence the stresses are evaluated at the Gauss points from which the generalized force and moment resultants are calculated and extrapolated to obtain the nodal values.

I. NUMERICAL EXAMPLES

The first two numerical examples are the benchmark problems used to validate the present approach. The first problem is about a simply supported stiffened rectangular plate with two orthogonal stiffeners and subjected to uniformly distributed load, which was solved by Sinha et al. (1992). The present results and those in the above reference are furnished as Fig. 5.

Since the results either on static deflections or forces/moments of stiffened conoidal shell are not available in the existing literature, the static results of simply supported unstiffened conoidal shell as obtained by the author are compared with those obtained by Hadid (1964) and Choi (1984) [Vide Fig. 6].

Additional problems on simply supported (SS) and clamped (CL) conoidal shell under central concentrated load are solved for different stiffener arrangements, depths and eccentricities.

1) Results and discussions

The results of the benchmark problems obtained by present method show good agreement with those presented by Sinha et al. (1992) and with those obtained by Hadid (1964) and Choi (1984) establishing the correctness of the present approach. The other problems, which are solved to explore the different aspects of bending behaviour of stiffened conoidal shells, are also checked for convergence and only converged results are reported. A particular shell action is taken to have converged for a particular finite element mesh if further refinement does not improve the result by more than one percent.

Effect of stiffener number and arrangement on deflection

From the results of Table 1 it is evident that as expected the stiffeners always play a positive role in arresting maximum deflections. When a single central stiffener (n_x =1 or n_y=1) or a pair of central stiffeners (n_x=n_y=1) is added to a bare shell the deflection is reduced drastically. When the number of stiffeners along x or y or along both the directions are increased the improvements of deflection are not that significant. It is interesting to note that for a given number of stiffeners and boundary condition the performances of curved y-stiffeners are found to be far better compared to that of the straight x-stiffeners. X-stiffened shells show deflections more than four and three times of that of y-stiffened shells for simply supported and clamped boundaries respectively. Providing stiffeners along both directions reduces deflections of y-stiffened shells further by 10 to 30%.

Effect of boundary condition on deflection

Clamped shells have more number of boundary constraints compared to the simply supported ones and hence the former is expected to yield lesser deflection. The results furnished in Table 1 reflect this tendency. For bare and x-stiffened shells the relative superiority of clamped boundary over simply supported one is very prominent. However, when y-stiffener or stiffeners along both the directions are provided the deflections for simply supported and clamped shells come close to one another. As for example with n_x=n_y=0 a simply supported shell exhibits a deflection 1.350 times of that of a clamped shell while the corresponding ratio is only 1.125 when n_x=n_y=3 and is 1.049 when n_x=n_y=5. Simply supported shells with stiffeners are often found to exhibit deflections less than clamped shells with no or fewer number of stiffeners. Hence the stiffeners can adequately make up the gap of rigidity between simply supported and clamped shells.

However, to specifically assess the performances of two shell options due weightage should be given to force and moment resultants apart from static deflections. Hence in the following sections the different force and moment resultants are presented and discussed in details.

Performances of combination of boundary conditions and stiffener arrangements with respect to different shell actions

The objective of this section is to look into the performances of different shell options combining different boundary conditions and stiffener arrangements on an overall basis considering force and moment resultants apart from static deflections. Tables 1 to 11 furnish the results of different shell actions which may be used as effective design charts for practicing engineers. Here upward deflection, tensile inplane force, hogging moment and inplane shear tending to rotate the shell anticlockwise are taken to be positive. At few points on the surfaces of stiffened conoidal shells positive deflections are also noted. But they are not reported due to their negligible magnitudes.

The best 3 shell combinations are selected from each of simply supported and clamped boundary conditions for the different shell actions and are arranged rankwise in ascending order of magnitude in Table 12 together with their points of occurrences. To designate the shell in the above table the boundary condition and the values of n_x and n_y are used, which means that a simply supported shell with no x-stiffener and one y-stiffener is represented by the symbol SS/0, 1. The results furnished in Tables 12

clearly shows that a particular shell combination which ranks high for a specific shell action may rank low or may not figure at all among the 6 selected configurations with respect to some other shell actions. The combination CL/5, 5 ranks first for $-\overline{w}$, ranks fifth for $\overline{M_x}$ and does not have any rank with respect to other shell actions like $\overline{N_x}$, $\overline{M_y}$ and so on.

Table 13 is derived from Table 12 and furnishes the number of times the different shell options appeared among the 6 selected configurations taking the best 3 from each boundary condition with respect to each of 11 shell actions It is also clear that shells with stiffeners along y-direction (occurring 22 times) are definitely better choices than those with stiffeners along x-direction (occurring 6 times). However, shells with biaxial stiffeners with 38 occurrences prove to be even better choices. It is also to be noted that bare shells do not occur among the first 6 options with respect to any of the shell actions and the number of occurrences for n=1 (includes n_x=1,n_y=0 and n_x=0,n_y=1 and n_x=n_y=1) is 22,that for n=3 (includes n_x=3,n_y=0 and n_x=0,n_y=3 and n_x=n_y=3) is 21 and that for n=5 (including n_x=5,n_y=0 and n_x=0,n_y=5 and n_x=n_y=5) is 23. These figures clearly establish the fact that n=3 or n=5 do not offer any significant improvement in the overall performances of stiffened conoidal shells compared to n=1 considering all the shell actions.

To conclusively select a particular shell configuration among the best two options i.e CL/3,3 and SS/5,5 each of which occur 7 times in Table 12 a relative performance matrix may be developed in a way explained below. Among the above two choices a value of 1 is assigned to the superior combination and 0 is assigned to the inferior combination with respect to the different shell actions. Both the shell options may be assigned a value of 1 if the value of a particular shell action for the relatively inferior shell option is not more than 10% of that of the relatively superior one. The relative performance matrix presented in Table 14 makes the CL/3,3 option as the better choice. Such matrices may be used to compare any two options when a designer has to take a firm decision regarding selection of one among the two possible configurations.

Effect of stiffener depth on different shell actions

To study the effect of stiffener depth on the different shell actions the h_s/h ratio is increased discretely from 0 to 10 for a clamped shell with n_x=n_y=3 and the results are furnished in Table 15.It is observed that 7 out of 11 shell actions exhibit a monotonic decreasing tendency with increase in stiffener depth. These shell actions include the deflection, sagging moments, which in the present case govern the shell depth. Departures from this general tendency are noted for tensile $\overline{N_x}$, $\overline{N_{xy}}$ and compressive $\overline{N_x}$ and $\overline{N_y}$. The critical compressive inplane forces which also have a role in determining the shell depth show decreasing tendency as h_s/h varies from 1 to 10 although these values exhibit an initial increasing tendency when a bare shell is stiffened with h_s/h =1. For positive $\overline{N_x}$ and

$\overline{N_{xy}}$ a decreasing tendency of the values with increase in h_s/h ratio is noticed in general although for some intermediate values of h_s/h this tendency is not strictly true. Since almost all of the shell actions exhibit improving tendency with increase in h_s/h ratio a maximum limit of the ratio may be assigned to 3 considering the functional requirements like aesthetics and headroom.

Effect of stiffener eccentricity on different shell actions

To study the effect of eccentricity on displacement, force and moment resultants a typical example of clamped shell with 3 stiffeners running in each direction having h_s/h =3 is taken up in the present section. The eccentricity is designated as positive or negative depending on whether the stiffener lies above or below the shell surface respectively. The eccentricity is zero when the mid surfaces of the shell and the stiffener coincide. It is observed from Table 16 that shells with positive or negative eccentricity exhibit almost equal values of all shell actions and hence a designer has the flexibility of providing the stiffeners above or below the shell surface being governed by functional requirements only. It is observed that eccentrically stiffened shells are better than concentrically stiffened ones in 7 out of 11 shell actions considered here including the transverse deflection and the moments which normally govern the shell depth. However, for compressive inplane forces, tensile $\overline{N_x}$ and $\overline{N_{xy}}$ the shell with e/h = 0 exhibits a better performance. The major inplane compressive force ($\overline{N_y}$) which also has a role in determining the shell depth shows the lowest value for e/h = 0 although the value is only 12.5% lower than the corresponding values for eccentrically stiffened shells. Hence judging the overall performances, eccentrically stiffened shells shall always be preferred if no functional restriction is violated.

It is also extremely interesting to note that the points of occurrences of the critical shell actions are identical whether eccentricity is positive, negative or zero in almost all cases. The few exceptions to this general trend are noted for

tensile $\overline{N_x}$ and hogging moments for concentrically stiffened shells only.

B. Conclusions

The following conclusions are drawn from the present study.

1. The finite element code used here is suitable for analysing static problems of stiffened conoids as this approach yields excellent results of the benchmark problems.
2. The curved stiffeners along y-direction are more efficient in reducing the deflections of conoids compared to the straight ones along x-direction.
3. For bare and x-stiffened shells the clamped edge gives much lesser deflections than the simply supported edge. When stiffeners are provided along y-direction or both directions the deflections of clamped and simply supported shells come relatively closer.
4. Among two shell configurations the one performing better in terms of static deflections may not be a better choice with respect to some other shell actions.
5. The increase in the stiffener depth causes an overall improvement of the static shell actions and the maximum limit of the stiffener depth shall be governed by functional requirements only.
6. Eccentrically stiffened shells are found to be better choices than the concentrically stiffened ones and whether the eccentricity of stiffeners is positive or negative matters very little.

REFERENCES

[1] Brebbia, C., and Hadid, H. A. 1971. Analysis of plates and shells using rectangular curved elements. CE/ 5/71. Civil Engineering Department, University of Southampton.

[2] Choi, C. K. 1984. A conoidal shell analysis by modified isoparametric element. Computers & Structures, 18(5): 921-924.

[3] Chakravorty, D., Bandyopadhyay, J. N., and Sinha, P. K. 1995. Free vibration analysis of point-supported laminated composite doubly curved shells – A finite element approach. Computers & Structures, 54(2): 191-198.

[4] Chakravorty, D., Bandyopadhyay, J. N., and Sinha, P. K. 1996. Finite element free vibration analysis of doubly curved laminated composite shells. Journal of Sound and Vibration,191(4): 491-504.

[5] Das, A. K., and Bandyopadhyay, J. N. 1993. Theoretical and experimental studies on conoidal shells. Computers & Structures, 49(3): 531-536.

[6] Ghosh, B. and Bandyopadhyay, J. N. 1989. Bending analysis of conoidal shell using curved quadratic isoparametric element. Computers & Structures, 33(3):717 – 728.

[7] Hadid, H. A. 1964. An analytical and experimental investigation into the bending theory of elastic conoidal shells. Ph. D. dissertation. University of Southampton.

[8] Nayak, A. N. and Bandopadhyay, J. N. 2002a. On the free vibration of stiffened shallow shells. Journal of Sound and Vibration, 255(2): 357-382.

[9] Nayak, A. N., and Bandopadhyay, J. N. 2002b April. Free vibration and design aids of stiffened conoidal shells. Journal of Engineering Mechanics, 128(4): 419-427.

[10] Prusty, B. G. and Satsangi, S. K. 2001. Analysis of stiffened shells for ships and ocean structures by finite element method. Ocean Engineering, 28: 621-638.

[11] Sinha, G. and Mukhopadhyay, M. 1995. Static and dynamic analysis of stiffened shells - a review. Proceedings of Indian National Science Academy, 61A(3-4): 195-219.

[12] Sinha, G., Sheikh. A. H., and Mukhopadhyay, M. 1992. A new finite element model for the analysis of arbitrary stiffened shells. Finite Elements in Analysis and Design, 12: 241-271.

List of symbols

a, b length and width of shell in plan

e eccentricities of both x and y direction stiffeners with respect to shell mid surface

E, G Young's modulus and shear modulus respectively

h, h_s shell thickness and stiffener thickness respectively

hh, hl higher and lower rise of conoidal shell

$\left.\begin{matrix} k_x, k_y, k_{xy} \\ k_{xz}\ k_{yz} \end{matrix}\right\}$ curvatures of shell

$\overline{M_x}, \overline{M_y}$ nondimensional moment resultants per unit length [=(M_x or M_y)/P]

$\overline{M_{xy}}$ nondimensional torsion resultant per unit length [=M_{xy} /P]

$\overline{N_x}, \overline{N_y}$ nondimensional inplane force resultants per unit length [=(a N_x or a N_y)/P]

$\overline{N_{xy}}$ nondimensional inplane shear resultant per unit length [= a N_{xy}/P]

n_x, n_y	number of stiffeners along x-direction and y-direction respectively
P	magnitude of concentrated load
q	magnitude of distributed load
Q_x , Q_y	transverse shear resultants of shell per unit length
R_y	radius of curvature of shell along y-direction
R_{xy}	radius of cross curvature of shell
u, v, w	displacements along x,y and z axes respectively
$\overline{w}$	nondimensional transverse deflection $[=wEh^3/Pa^2]$
w_s	width of stiffener
α, β	rotations vectorially along y and x axes respectively
ε_x , ε_y	normal strains
γ_{xy} , γ_{xz}, γ_{yz}	shear strains
υ	Poisson's ratio
ξ , η	local natural coordinates of an element
σ_x , σ_y	normal stresses
τ_{xy} , τ_{xz}, τ_{yz}	shear stresses

Table 1: Maximum values of nondimensional downward deflection ($\overline{-w}$) of stiffened conoids under central point load

Stiffener arrangement	Along x-direction ($n_x = n, n_y=0$)		Along y-direction ($n_x =0, n_y=n$)		Along both x and y directions ($n_x = n_y = n$)	
Edge condition	SS	CL	SS	CL	SS	CL
n = 0	-0.119×10^{-1} (0.50,0.50)	-0.881×10^{-2} (0.50,0.50)	-0.119×10^{-1} (0.50,0.50)	-0.881×10^{-2} (0.50,0.50)	-0.119×10^{-1} (0.50,0.50)	-0.881×10^{-2} (0.50,0.50)
n = 1	-0.984×10^{-2} (0.50,0.50)	-0.669×10^{-2} (0.50,0.50)	-0.0221×10^{-2} (0.50,0.50)	-0.205×10^{-2} (0.50,0.50)	-0198×10^{-2} (0.50,0.50)	-0176×10^{-2} (0.54,0.50)
n = 3	-0.930×10^{-2} (0.50,0.50)	-0.656×10^{-2} (0.50,0.50)	-0.212×10^{-2} (0.50,0.50)	-0.202×10^{-2} (0.50,0.50)	-0.175×10^{-2} (0.50,0.50)	-0.163×10^{-2} (0.50,0.50)
n = 5	-0.869×10^{-2} (0.50,0.50)	-0.617×10^{-2} (0.50,0.50)	-0.203×10^{-2} (0.50,0.50)	-0.196×10^{-2} (0.50,0.50)	-0.149×10^{-2} (0.50,0.50)	-0142×10^{-2} (0.50,0.50)

a/b=1, a/h=100, a/w_s=50, h_s/h = 2, a/hh =5 , a/hl=20, υ = 0.3

For all the cases the eccentricities of stiffeners are negative.

The values in parentheses indicate the nondimensional coordinates (x/*a*,y/*b*) of the points of occurrences of maximum shell actions.

Table 2: Maximum values of nondimensional tensile inplane force ($\overline{N_x}$) of stiffened conoids under central point load

Stiffener arrangement	Along x-direction ($n_x = n, n_y=0$)		Along y-direction ($n_x =0, n_y=n$)		Along both x and y directions ($n_x = n_y = n$)	
Edge condition	SS	CL	SS	CL	SS	CL
n = 0	4.260 (0.25, 0.08)	4.499 (0.00,0.50)	4.260 (0.25, 0.08)	4.499 (0.00,0.50)	4.260 (0.25, 0.08)	4.499 (0.00,0.50)
n = 1	4.221 (0.25, 0.08)	6.492 (0.00,0.50)	0.465 (0.17,0.06)	0.622 (0.00,0.50)	0.594 (0.17,0.08)	1.193 (0.00,0.50)
n = 3	3.669 (0.25, 0.08)	6.218 (0.00,0.50)	0.112 (0.42,0.25)	0.342 (0.42,0.25)	2.172 (0.25,0.50)	2.107 (0.25,0.50)
n = 5	3.708 (0.25, 0.08)	5.815 (0.00,0.50)	0.117 (0.42,0.25)	0.306 (0.42,0.25)	3.057 (0.33.,050)	3.016 (0.33,0.50)

a/b=1, a/h=100, a/w_s=50, h_s/h = 2, a/hh =5 , a/hl=20, υ = 0.3

For all the cases the eccentricities of stiffeners are negative.

The values in parentheses indicate the nondimensional coordinates (x/*a*,y/*b*) of the points of occurrences of maximum shell actions.

Table 3: Maximum values of nondimensional tensile inplane force ($\overline{N_y}$) of stiffened conoids under central point load

Stiffener arrangement	Along x-direction ($n_x = n, n_y=0$)		Along y-direction ($n_x =0, n_y=n$)		Along both x and y directions ($n_x = n_y = n$)	
Edge condition	SS	CL	SS	CL	SS	CL
n = 0	2.878 (0.33,0.50)	2.041 (0.33,0.50)	2.878 (0.33,0.50)	2.041 (0.33,0.50)	2.878 (0.33,0.50)	2.041 (0.33,0.50)
n = 1	1.169 (0.08,0.08)	2.038 (0.00,0.50)	0.757 (0.25,0.59)	0.776 (0.25,0.59	0.371 (0.25,0.17)	0.409 (0.00,0.50)
n = 3	1.060 (0.08,0.08)	1.910 (0.00,0.50)	1.640 (0.25,0.59	1.082 (0.25,0.59)	1.127 (0.25,0.42)	0.581 (0.25,0.42)
n = 5	0.983 (0.08,0.08)	1.842 (0.00,0.50)	1.548 (0.33,0.42)	1.111 (0.33,0.42)	0.767 (0.25,0.59	0.485 (0.17,0.50)

a/b=1, a/h=100, a/w_s=50, h_s/h = 2, a/hh =5 , a/hl=20, υ = 0.3

For all the cases the eccentricities of stiffeners are negative.

The values in parentheses indicate the nondimensional coordinates (x/*a*,y/*b*) of the points of occurrences of maximum shell actions.

Table 4: Maximum values of nondimensional anticlockwise inplane shear ($\overline{N_{xy}}$) of stiffened conoids under central point load

Stiffener arrangement	Along x-direction (n_x = n, n_y=0)		Along y-direction (n_x =0, n_y=n)		Along both x and y directions (n_x = n_y = n)	
Edge condition	SS	CL	SS	CL	SS	CL
n = 0	5.954 (0.08,0.00)	5.697 (0.42,0.33)	5.954 (0.08,0.00)	5.697 (0.42,0.33)	5.954 (0.08,0.00)	5.697 (0.42,0.33)
n = 1	5.973 (0.08,0.00)	4.221 (0.42,0.33)	2.265 (0.46,0.42)	2.288 (0.46,0.42)	2.324 (0.46,0.42)	2.284 (0.46,0.42)
n = 3	5.124 (0.08,0.00)	4.017 (0.33,0.25)	2.201 (0.46,0.42)	2.232 (0.46,0.42)	2.116 (0.46,0.42)	2.138 (0.46,0.42)
n = 5	4.654 (0.08,0.00)	3.781 (0.42,0.33)	2.021 (0.46,0.42)	2.055 (0.46,0.42)	1.747 (0.46,0.42)	1.776 (0.46,0.42)

a/b=1, a/h=100, a/w_s=50, h_s/h = 2, a/hh =5 , a/hl=20, υ = 0.3

For all the cases the eccentricities of stiffeners are negative.

The values in parentheses indicate the nondimensional coordinates (x/*a*,y/*b*) of the points of occurrences of maximum shell actions.

Table 5: Maximum values of nondimensional hogging moment ($\overline{M_x}$) of stiffened conoids under central point load

Stiffener arrangement	Along x-direction (n_x = n, n_y=0)		Along y-direction (n_x =0, n_y=n)		Along both x and y directions (n_x = n_y = n)	
Edge condition	SS	CL	SS	CL	SS	CL
n = 0	0.177×10^{-1} (0.42,0.50)	0.240×10^{-1} (0.42,0.50)	0.177×10^{-1} (0.42,0.50)	0.240×10^{-1} (0.42,0.50)	0.177×10^{-1} (0.42,0.50)	0.240×10^{-1} (0.42,0.50)
n = 1	0.153×10^{-1} (0.42,0.25)	0.129×10^{-1} (0.42,0.42)	0.108×10^{-1} (0.42,0.50)	0.119×10^{-1} (0.42,0.50)	0.324×10^{-2} (0.42,0.33)	0.455×10^{-2} (0.42,0.33)
n = 3	0.128×10^{-1} (0.42,0.17)	0.109×10^{-1} (0.50,0.25)	0.111×10^{-1} (0.42,0.50)	0.118×10^{-1} (0.42,0.50)	0.445×10^{-2} (0.25,0.50)	0.473×10^{-2} (0.42,0.33)
n = 5	0.112×10^{-1} (0.42,0.17)	0.105×10^{-1} (0.00,0.42)	0.141×10^{-1} (0.33,0.50)	0.133×10^{-1} (0.33,0.50)	0.592×10^{-2} (0.33,0.50)	0.584×10^{-2} (0.33,0.50)

a/b=1, a/h=100, a/w_s=50, h_s/h = 2, a/hh =5 , a/hl=20, υ = 0.3

For all the cases the eccentricities of stiffeners are negative.

The values in parentheses indicate the nondimensional coordinates (x/*a*,y/*b*) of the points of occurrences of maximum shell actions.

Table 6: Maximum values of nondimensional hogging moment ($\overline{M_y}$) of stiffened conoids under central point load

Stiffener arrangement	Along x-direction ($n_x = n, n_y=0$)		Along y-direction ($n_x =0, n_y=n$)		Along both x and y directions ($n_x = n_y = n$)	
Edge condition	SS	CL	SS	CL	SS	CL
n = 0	0.334×10^{-1} (0.50,0.28)	0.356×10^{-1} (0.50,0.33)	0.334×10^{-1} (0.50,0.28)	0.356×10^{-1} (0.50,0.33)	0.334×10^{-1} (0.50,0.28)	0.356×10^{-1} (0.50,0.33)
n = 1	0.304×10^{-1} (0.46,0.25)	0.288×10^{-1} (0.50,0.33)	0.376×10^{-2} (0.42,0.33)	0.442×10^{-2} (0.42,0.33)	0.423×10^{-2} (0.42,0.33)	0.528×10^{-2} (0.42,0.33)
n = 3	0.291×10^{-1} (0.50,0.29)	0.301×10^{-1} (0.50,0.33)	0.412×10^{-2} (0.42,0.33)	0.444×10^{-2} (0.42,0.33)	00.522×10^{-2} (0.42,0.33)	0.580×10^{-2} (0.42,0.33)
n = 5	0.249×10^{-1} (0.50,0.33)	0.295×10^{-1} (0.50,0.33)	0.356×10^{-2} (0.42,0.33)	0.382×10^{-2} (0.42,0.33)	0.427×10^{-2} (0.42,0.33)	0.479×10^{-2} (0.42,0.42)

a/b=1, a/h=100, a/w_s=50, h_s/h = 2, a/hh =5 , a/hl=20, υ = 0.3

For all the cases the eccentricities of stiffeners are negative.

The values in parentheses indicate the nondimensional coordinates (x/*a*,y/*b*) of the points of occurrences of maximum shell actions.

Table 7: Maximum values of nondimensional anticlockwise torsion ($\overline{M_{xy}}$) of stiffened conoids under central point load

Stiffener arrangement	Along x-direction ($n_x = n, n_y=0$)		Along y-direction ($n_x =0, n_y=n$)		Along both x and y directions ($n_x = n_y = n$)	
Edge condition	SS	CL	SS	CL	SS	CL
n = 0	0.251×10^{-1} (0.42,0.42)	0.232×10^{-1} (0.42,0.42)	0.251×10^{-1} (0.42,0.42)	0.232×10^{-1} (0.42,0.42)	0.251×10^{-1} (0.42,0.42)	0.232×10^{-1} (0.42,0.42)
n = 1	01421×10^{-1}. (0.42,0.42)	0.127×10^{-1} (0.42,0.42)	0.473×10^{-2} (0.42,0.42)	0.446×10^{-2} (0.42,0.42)	0.292×10^{-2} (0.33,0.42)	0.283×10^{-2} (0.33,0.42)
n = 3	0.135×10^{-1} (0.42,0.42)	0.123×10^{-1} (0.42,0.42)	0.496×10^{-2} (0.42,0.42)	0.449×10^{-2} (0.42,0.42)	0.362×10^{-2} (0.33,0.42)	0.372×10^{-2} (0.33,0.42)
n = 5	0.134×10^{-1} (0.42,0.42)	0.124×10^{-1} (0.42,0.42)	0.601×10^{-2} (0.42,0.42)	0.3599×10^{-2} (0.42,0.42)	0.451×10^{-2} (0.42,0.42)	0.453×10^{-2} (0.42,0.42)

a/b=1, a/h=100, a/w_s=50, h_s/h = 2, a/hh =5 , a/hl=20, υ = 0.3

For all the cases the eccentricities of stiffeners are negative.

The values in parentheses indicate the nondimensional coordinates (x/*a*,y/*b*) of the points of occurrences of maximum shell actions.

Table 8: Maximum values of nondimensional inplane compressive force ($\overline{-N_x}$) of stiffened conoids under central point load

Stiffener arrangement	Along x-direction ($n_x = n.n_y=0$)		Along y-direction ($n_x =0$, $n_y=n$)		Along both x and y directions ($n_x = n_y = n$)	
Edge condition	SS	CL	SS	CL	SS	CL
n = 0	-0.156×10^{2} (0.50,0.50)	-0.107×10^{2} (0.50,0.50)	-0.156×10^{2} (0.50,0.50)	-0.107×10^{2} (0.50,0.50)	-0.156×10^{2} (0.50,0.50)	-0.107×10^{2} (0.50,0.50)
n = 1	-0.294×10^{2} (0.50,0.50)	-0.248×10^{2} (0.50,0.50)	-0.380×10^{1} (0.42,0.50)	-0.335×10^{1} (0.42,0.50)	-0.741×10^{1} (0.50,0.50)	-0.756×10^{1} (0.50,0.50)
n = 3	-0.286×10^{2} (0.50,0.50)	-0.245×10^{2} (0.50,0.50)	-0.382×10^{1} (0.42,0.50)	-0.354×10^{1} (0.42,0.50)	-0.890×10^{1} (0.50,0.50)	-0.882×10^{1} (0.50,0.50)
n = 5	-0.278×10^{2} (0.50,0.50)	-0.239×10^{2} (0.50,0.50)	-0.363×10^{1} (0.42,0.50)	-0.350×10^{1} (0.42,0.50)	-0.101×10^{2} (0.50,0.50)	-0.101×10^{2} (0.50,0.50)

a/b=1, a/h=100, a/w_s=50, h_s/h = 2, a/hh =5 , a/hl=20, υ = 0.3

For all the cases the eccentricities of stiffeners are negative.

The values in parentheses indicate the nondimensional coordinates (x/*a*,y/*b*) of the points of occurrences of maximum shell actions.

Table 9: Maximum values of nondimensional compressive inplane force ($\overline{-N_y}$) of stiffened conoids under central point load

Stiffener arrangement	Along x-direction (n_x = n, n_y=0)		Along y-direction (n_x =0, n_y=n)		Along both x and y directions (n_x = n_y = n)	
Edge condition	SS	CL	SS	CL	SS	CL
n = 0	-0.225×10^{2} (0.50,0.50)	-0.231×10^{2} (0.50,0.50)	-0.225×10^{2} (0.50,0.50)	-0.231×10^{2} (0.50,0.50)	-0.225×10^{2} (0.50,0.50)	-0.231×10^{2} (0.50,0.50)
n = 1	-0.115×10^{2} (0.50,0.42)	-0.123×10^{2} (0.50,0.42)	-0.272×10^{2} (0.50,0.50)	-0.284×10^{2} (0.50,0.50)	-0.211×10^{1} (0.50,0.50)	-0.219×10^{1} (0.50,0.50)
n = 3	-0.116×10^{2} (0.50,0.42)	-0.123×10^{2} (0.50,0.42)	-0.281×10^{2} (0.50,0.50)	-0.287×10^{2} (0.50,0.50)	-0.210×10^{1} (0.50,0.50)	-0.214×10^{1} (0.50,0.50)
n = 5	-0.112×10^{2} (0.50,0.42)	-0.119×10^{2} (0.50,0.42)	-0.284×10^{2} (0.50,0.50)	-0.289×10^{2} (0.50,0.50)	-0.198×10^{2} (0.50,0.50)	-0.202×10^{2} (0.50,0.50)

a/b=1, a/h=100, a/w_s=50, h_s/h = 2, a/hh =5 , a/hl=20, υ = 0.3

For all the cases the eccentricities of stiffeners are negative.

The values in parentheses indicate the nondimensional coordinates (x/*a*,y/*b*) of the points of occurrences of maximum shell actions.

Table10: Maximum values of nondimensional sagging moment ($\overline{-M_x}$) of stiffened conoids under central point load

Stiffener arrangement	Along x-direction ($n_x = n, n_y=0$)		Along y-direction ($n_x =0, n_y=n$)		Along both x and y directions ($n_x = n_y = n$)	
Edge condition	SS	CL	SS	CL	SS	CL
n = 0	-0.215 (0.50,0.50)	-0.210 (0.50,0.50)	-0.215 (0.50,0.50)	-0.210 (0.50,0.50)	-0.215 (0.50,0.50)	-0.210 (0.50,0.50)
n = 1	-0.802×10^{-1} (0.50,0.50)	-0.746×10^{-1} (0.50,0.50)	-0.531×10^{-1} (0.50,0.50)	-0.560×10^{-1} (0.50,0.50)	-0.163×10^{-1} (0.50,0.50)	-0.172×10^{-1} (0.50,0.50)
n = 3	-0.791×10^{-1} (0.50,0.50)	-0.742×10^{-1} (0.33,0.25)	-0.566×10^{-1} (0.50,0.50)	-0.580×10^{-1} (0.50,0.50)	-0.189×10^{-1} (0.50,0.50)	-0.191×10^{-1} (0.50,0.50)
n = 5	-0.775×10^{-1} (0.50,0.50)	-0.732×10^{-1} (0.50,0.50)	-0.619×10^{-1} (0.50,0.50)	-0.624×10^{-1} (0.50,0.50)	-0.208×10^{-1} (0.50,0.50)	-0.208×10^{-1} (0.50,0.50)

a/b=1, a/h=100, a/w_s=50, h_s/h = 2, a/hh =5 , a/hl=20, υ = 0.3

For all the cases the eccentricities of stiffeners are negative.

The values in parentheses indicate the nondimensional coordinates (x/*a*,y/*b*) of the points of occurrences of maximum shell actions.

Table11: Maximum values of nondimensional sagging moment ($-\overline{M_y}$) of stiffened conoids under central point load

Stiffener arrangement	Along x-direction ($n_x = n, n_y=0$)		Along y-direction ($n_x =0, n_y=n$)		Along both x and y directions ($n_x = n_y = n$)	
Edge condition	SS	CL	SS	CL	SS	CL
n = 0	-0.250 (0.50,0.50)	-0.238 (0.50,0.50)	-0.250 (0.50,0.50)	-0.238 (0.50,0.50)	-0.250 (0.50,0.50)	-0.238 (0.50,0.50)
n = 1	-0.144 (0.50,0.50)	-0.132 (0.50,0.50)	-0.381×10^{-1} (0.50,0.50)	-0.389×10^{-1} (0.50,0.50)	-0.230×10^{-1} (0.50,0.50)	-0.228×10^{-1} (0.54,0.50)
n = 3	-0.143 (0.50,0.50)	-0.133 (0.50,0.50)	-0.384×10^{-1} (0.50,0.50)	-0.393×10^{-1} (0.50,0.50)	-0.227×10^{-1} (0.50,0.50)	-0.226×10^{-1} (0.50,0.50)
n = 5	-0.141 (0.50,0.50)	-0.132 (0.50,0.50)	-0.401×10^{-1} (0.50,0.50)	-0.403×10^{-1} (0.50,0.50)	-0.221×10^{-1} (0.50,0.50)	-0.220×10^{-1} (0.50,0.50)

a/b=1, a/h=100, a/w_s=50, h_s/h = 2, a/hh =5 , a/hl=20, υ = 0.3

For all the cases the eccentricities of stiffeners are negative.

The values in parentheses indicate the nondimensional coordinates (x/*a*,y/*b*) of the points of occurrences of maximum shell actions.

Table12: Shell configurations arranged according to ascending order of the values of shell actions taking best three options from each boundary condition.

Shell actions	Points of occurrences (x/a, y/b)	Shell configurations
$\overline{-w}$	(0.50,0.50)	CL/5,5
	(0.50,0.50)	SS5,5
	(0.50,0.50)	CL/3,3
	(0.50,0.50)	SS/3,3
	(0.50,0.50)	CL/1,1
	(0.50,0.50)	SS/1,1
$\overline{N_x}$	(0.42,0.25)	SS/0,3
	(0.42,0.25)	SS/0,5
	(0.42,0.25)	CL/0,5
	(0.42,0.25)	CL/0,3
	(0.17,0.08)	SS/0,1
	(0.00,0.50)	CL/0,1
$\overline{N_y}$	(0.25,0.17)	SS/1,1
	(0.0.0,0.50)	CL/1,1
	(0.17,0.50)	CL/5,5
	(0.25,0.50)	CL/3,3
	(0.25,0.42)	SS/0,1
	(0.25,0.50)	SS/5,5
$\overline{N_{xy}}$	(0.46,0.42)	SS/5,5
	(0.46,0.42)	CL/5,5
	(0.46,0.42)	SS//0,5
	(0.46,0.42)	CL/0,5
	(0.46,0.42)	SS/3,3

	(0.46,0.42)	CL/3,3
$\overline{M_x}$	(0.42,0.33)	SS/1,1
	(0.25,0.50)	SS/3,3
	(0.42,0.33)	CL/1,1
	(0.42,0.33)	CL/3,3
	(0.33,0.50)	CL/5,5
	(0.33,0.50)	SS/5,5
$\overline{M_y}$	(0.42,0.33)	SS/0,5
	(0.42,0.33)	SS/0,1
	(0.42,0.33)	CL/0,5
	(0.42,0.33)	SS/0,3
	(0.42,0.33)	CL/0,1
	(0.42,0.33)	CL/0,3
$\overline{M_{xy}}$	(0.33,0.42)	CL/1,1
	(0.33,0.42)	SS/1,1
	(0.33,0.42)	SS/3,3
	(0.33,0.42)	CL/3,3
	(0.42,0.42)	CL/0,1
	(0.42,0.42)	SS/5,5
$\overline{-N_x}$	(0.42,0.50)	CL/0,1
	(0.42,0.50)	CL/0,5
	(0.42,0.50)	CL/0,3
	(0.42,0.50)	SS/0,5
	(0.42,0.50)	SS/0,1
	(0.42,0.50)	SS/0,3

Table12: Continued

$\overline{-N_y}$	(0.50,0.42)	SS/5,0
	(0.50,0.42)	SS/1,0
	(0.50,0.42)	SS/3,0
	(0.50,0.42)	CL/5,0
	(0.50,0.42)	CL/1,0
	(0.50,0.42)	CL/3,0
$\overline{-M_x}$	(0.50,0.50)	SS/1,1
	(0.50,0.50)	CL/1,1
	(0.50,0.50)	SS/3,3
	(0.50,0.50)	CL/3,3
	(0.50,0.50)	SS/5,5
	(0.50,0.50)	CL/5,5
$\overline{-M_y}$	(0.50,0.50)	CL/5,5
	(0.50,0.50)	SS/5,5
	(0.50,0.50)	CL/3,3
	(0.50,0.50)	SS/3,3
	(0.50,0.50)	CL/1,1
	(0.50,0.50)	SS/1,1

Table13: Number of occurrences of different shell configurations in Table 12

Stiffener arrangement	Along x-direction (n_x = n, n_y=0)		Along y-direction (n_x =0, n_y=n)		Along both x and y directions (n_x = n_y = n)	
Edge condition	SS	CL	SS	CL	SS	CL
n = 0	0	0	0	0	0	0
n = 1	1	1	4	4	6	6
n = 3	1	1	3	3	6	7
n = 5	1	1	4	4	7	6
Total	3	3	11	11	19	19

Table14: Relative performance matrix considering CL/3,3 and SS/5,5 shell configurations

Shell Actions	SS/5,5	CL/3,3
$\overline{-w}$	1	1
$\overline{N_x}$	0	1
$\overline{N_y}$	0	1
$\overline{N_{xy}}$	1	0
$\overline{M_x}$	0	1
$\overline{M_y}$	1	0
$\overline{M_{xy}}$	0	1
$\overline{-N_x}$	0	1
$\overline{-N_y}$	1	1

$\overline{-M_x}$	1	1
$\overline{-M_y}$	1	1
Total	6	9

Table15: Maximum values of nondimensional shell actions of stiffened conoid (CL/3,3) for different stiffener depths

II. SHELL ACTIONS	**III. H_S/H = 0**	**IV. H_S/H = 1**	**V. H_S/H = 2**	**VI. H_S/H = 3**	**VII. H_S/H = 5**	**VIII. H_S/H = 10**
$\overline{-w}$	-0.882×10^{-2}	-0.298×10^{-2}	-0.163×10^{-2}	-0.106×10^{-2}	-0.585×10^{-3}	-0.234×10^{-3}
	(0.50,0.50)	(0.50,0.50)	(0.50,0.50)	(0.50,0.50	(0.50,0.50)	(0..50,0.50)
$\overline{N_x}$	0.450×10^{1}	0.174×10^{1}	0.211×10^{1}	0.213×10^{1}	0.171×10^{1}	0.801
	(0.00,0.50)	(0.35,0.50)	(0,25,0.50)	0.25,0.50	(0.25,0.50)	(0.25,0.50)
$\overline{N_y}$	0.204×10^{1}	0.107×10^{1}	0.581	0.265	0.108	0.575
	(0.33,0.50)	(0.25,0.42)	(0.25,0.42)	(0.16,0.50)	(0.25,0.00)	(0.50,0.00)
$\overline{N_{xy}}$	0.570×10^{1}	0.197×10^{1}	0.214×10^{1}	0.194×10^{1}	0.146×10^{1}	0.815
	(0.42,0.33)	(0.33,0.33)	(0.46,0.42)	(0.46,0.42)	(046,0.42)	(0.46,0.42)
$\overline{M_x}$	0.240×10^{-1}	0.662×10^{-2}	0.473×10^{-2}	0.382×10^{-2}	0.279×10^{-2}	0.168×10^{-2}
	(0.42,0.50)	(0.25,0.50)	(0.42,0.33)	(0.42,0.33)	(0.42,0.33)	(0.42,0.42)
$\overline{M_y}$	0.357×10^{-1}	0.994×10^{-2}	0.580×10^{-2}	0.411×10^{-2}	0.317×10^{-2}	0.188×10^{-2}
	(0.50,0.33)	((0.42,0.33)	(0.42,0.33)	(0.42,0.33)	(0.42,0.42)	(0.42,0.42)

$\overline{M_{xy}}$	0.232×10^{-1}	0.737×10^{-2}	0.372×10^{-2}	0.255×10^{-2}	0.150×10^{-2}	0.693×10^{-3}
	(0.42,0.42)	((0.42,0.42)	(0.42,0.33)	(0.33,0.42)	(0.33,0.42)	(0.33,0.42)
$\overline{-N_x}$	-0.107×10^{2}	-0.118×10^{2}	-0.882×10^{1}	-0.703×10^{1}	-0.514×10^{1}	-0.304×10^{1}
	(0.50,0.500	(0.50,0.50)	(0.50,0.50)	(0.50,0.50)	(0.50,0.50)	(050,0.50)
$\overline{-N_y}$	-0.231×10^{2}	-0.284×10^{2}	-0.214×10^{2}	-0.164×10^{2}	-0.107×10^{2}	-0.533×10^{1}
	(0.50,0.50)	(0.66,0.33)	(0.50,0.50)	(0.50,0.50)	(0.50,0.50)	(0.50,0.50)
$\overline{-M_x}$	-0.209	-0.519×10^{-1}	-0.191×10^{-1}	-0.108×10^{-1}	-0.715×10^{-2}	-0.356×10^{-2}
	(0.50,0.50)	(0.50,0.50)	(0.50,0.50)	(0.50,0.42)	(050,0.42)	(050,0.42)
$\overline{-M_y}$	-0.238	-0.602×10^{-1}	-0.226×10^{-1}	-0.151×10^{-1}	-0.939×10^{-2}	-0.445×10^{-2}
	(0.50,0.50)	(0.50,0.50)	(0.50,0.50)	(0.58,0.50)	(0.58,0.50)	(058,0.50)

a/b=1, a/h=100, a/w_s=50, a/hh =5 , a/hl=20, υ = 0.3

For all the cases the eccentricities of stiffeners are negative.

The values in parentheses indicate the nondimensional coordinates (x/*a*,y/*b*) of the points of occurrences of maximum shell actions.

Table 16: Maximum values of nondimensional shell actions of stiffened conoid (CL/3,3) for different stiffener eccentricities

IX.	XI. ECCENTRICITY VALUES		
X. SHELL ACTIONS	XII. E/H = -2	XIII. E/H = 0	XIV. E/H = +2
$\overline{-w}$	-0.106×10^{-2}	-0.170×10^{-2}	-0.107×10^{-2}
	(0.50, 0.50)	(0.50, 0.50)	(0.50, 0.50)
$\overline{N_x}$	0.213×10^{1}	0.341	0.212×10^{1}
	(0.25,0.50)	(0.42,0.17)	(0.25,0.50)
$\overline{N_y}$	0.265	0.525	0.259
	(0.17,0.50)	(0.17,0.50)	(0.17,0.50)
$\overline{N_{xy}}$	0.194×10^{1}	0.140×10^{1}	0.199×10^{1}
	(0.46,0.42)	(0.46,0.42)	(0.46,0.42)
$\overline{M_x}$	0.383×10^{-2}	0.489×10^{-2}	0.382×10^{-2}
	(0.42,0.33)	(0.42,0.33)	(0.42,0.33)
$\overline{M_y}$	0.411×10^{-2}	0.655×10^{-2}	0.412×10^{-2}
	(0.42,0.33)	(0.42,0.33)	(0.42,0.33)
$\overline{M_{xy}}$	0.255×10^{-2}	0.388×10^{-2}	0.256×10^{-2}
	(0.33,0.42)	(0.33,0.42)	(0.33,0.42)

$\overline{-N_x}$	-0.703×10^{1}	-0.237×10^{1}	-0.705×10^{1}
	(0.50,0.50)	(0.50,0.50)	(0.50,0.50)
$\overline{-N_y}$	-0.164×10^{2}	-0.145×10^{2}	-0.168×10^{2}
	(0.50,0.50)	(0.50,0.50)	(0.50,0.50)
$\overline{-M_x}$	-0.108×10^{-1}	-0.191×10^{-1}	-0.108×10^{-1}
	(0.50,0.42)	(0.50,0.50)	(0.50,0.42)
$\overline{-M_y}$	-0.151×10^{-1}	-0.230×10^{-1}	-0.152×10^{-1}
	(0.58,0.50)	(0.46,0.50)	(0.58,0.50)

a/b=1, a/h=100, a/w_s=50, h_s/h=3,hh/a = 5, hl/a = 20, υ = 0.3

The values in parentheses indicate the nondimensional coordinates (x/*a*,y/*b*) of the points of occurrences of maximum shell actions.

List of figure captions

Fig 1: Conoidal shell with eccentric stiffeners

Fig 2: Isoparametric elements

(a) 8 noded shell element

(b) 3 noded x-stiffener element

(c) 3 noded y-stiffener element

Fig 3: Nodal degrees of freedom

Fig 4: Generalised force and moment resultants

Fig.5 (a) Deflection of concentrically stiffened plate at x = 0.19m

(b) Moment of concentrically stiffened plate at y = 0.38m

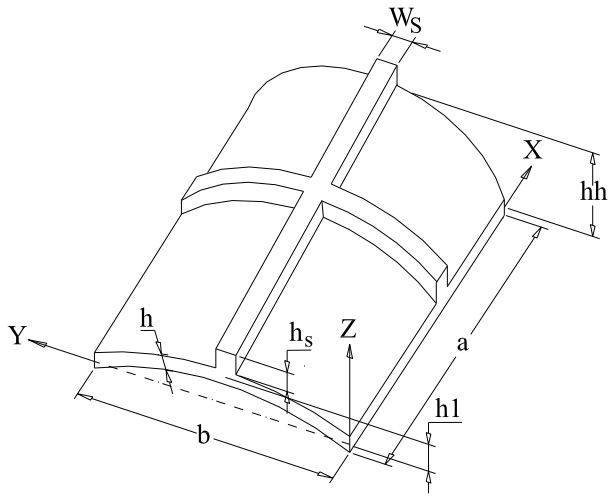
(c) Deflection of eccentrically stiffened plate at x = 0.19m

(d) Moment of eccentrically stiffened plate at x = 0.38m

Fig.6 (a) Values of deflection of unstiffened conoidal shell at y/b = 1/2

(b) Values of inplane force of unstiffened conoidal shell at y/b = 1/2

Fig 1: Conoidal shell with eccentric stiffeners



$$z = 4\left[hl + (hh - hl)\frac{x}{a} \right]\left[\frac{y}{b} - \frac{y^2}{b^2} \right]$$

Fig 2: Isoparametric elements

(a) 8 noded shell element
(b) 3 noded x-stiffener element
(c) 3 noded y-stiffener element

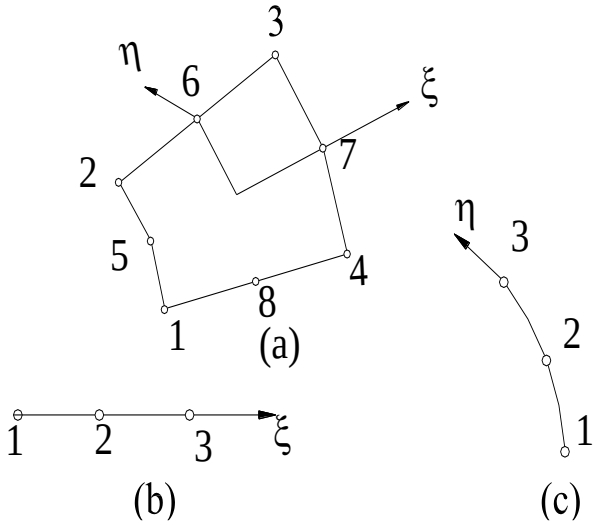


Fig 3: Nodal degrees of freedom

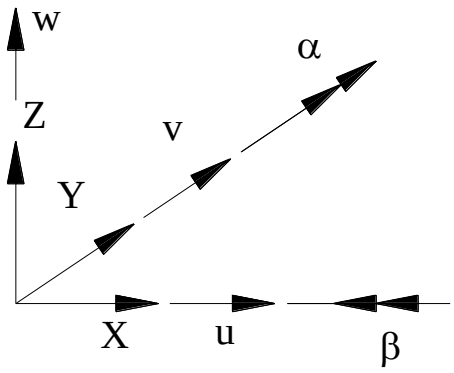


Fig 4: Generalised force and moment resultants

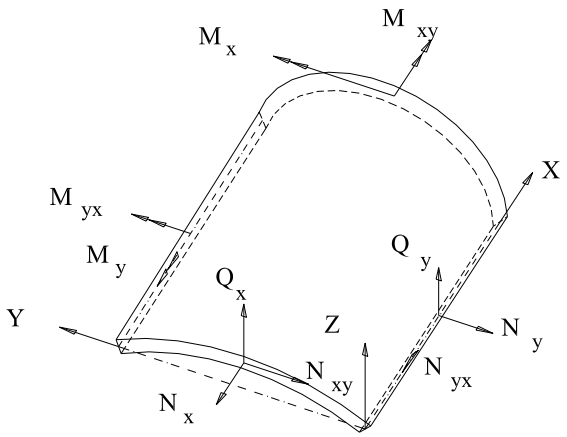


Fig.5 (a) Deflection of concentrically stiffened plate at x = 0.19m

(b) Moment of concentrically stiffened plate at y = 0.38m

(c) Deflection of eccentrically stiffened plate at x = 0.19m

(d) Moment of eccentrically stiffened plate at x = 0.38m

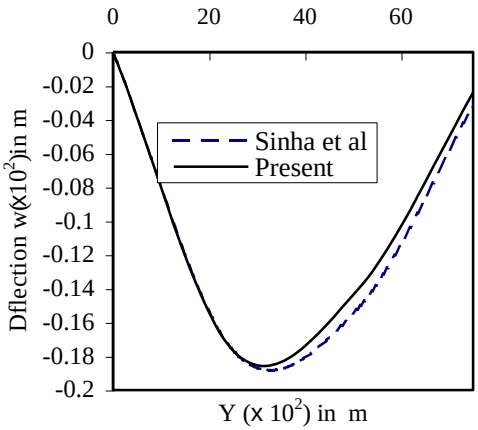


Fig.5 (a)

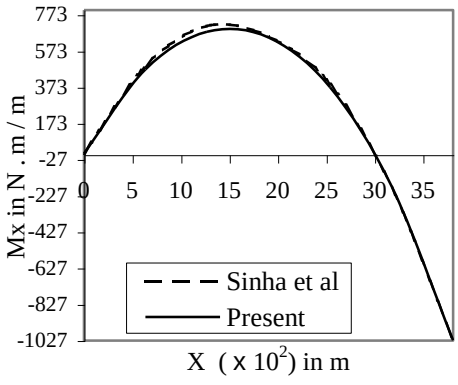


Fig.5 (b)

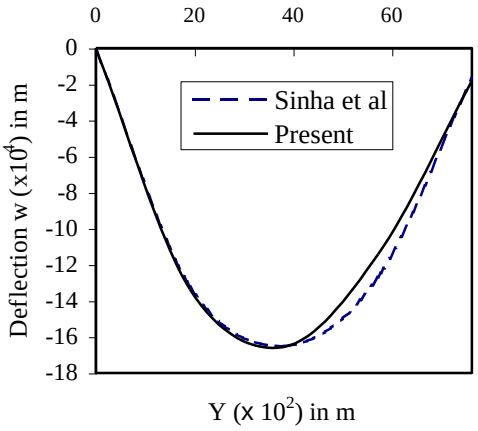


Fig.5(c)

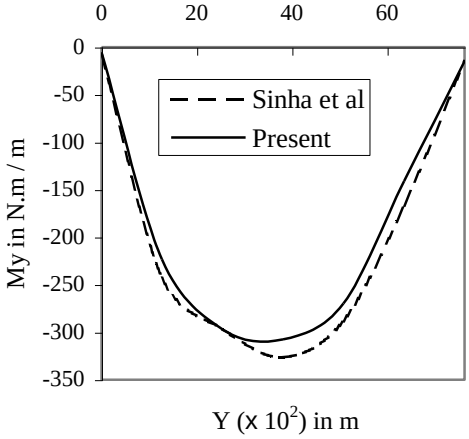


Fig.5 (d)

Simply supported plate details: a = 0.76m, b = 1.52m, h = 0.64m, x-stiffener size: 0.013m×0.13m, y-stiffener size: 0.013m×0.076m, E =2.069 ×10^{8} kN/m^{2}, υ = 0.3, q = 68.975 kN/m^{2}.

Fig.6 (a) Values of deflection at y/b = 1/2

(b) Values of inplane force at y/b = 1/2

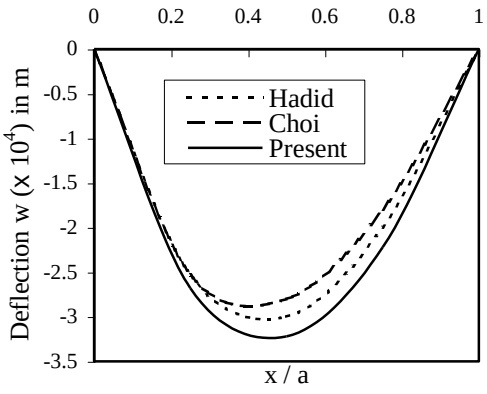


Fig.6 (a)

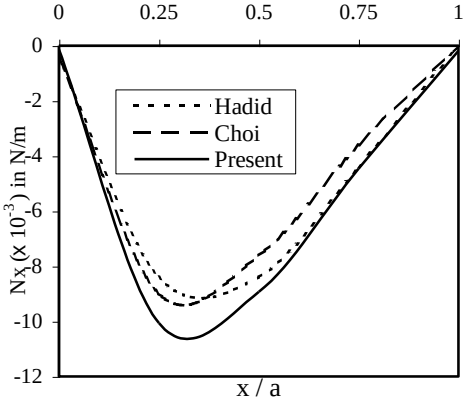


Fig.6 (b)

Simply supported conoidal shell details: a =1.83m, b = 2.51m, hh = 0.46m, hl = 0.23m, h = 0.013m,

E = 0.396 ×10^{8} kN/m^{2,} υ = 0.15, q = 2.9356 kN/m^{2}